# Supplementary Information

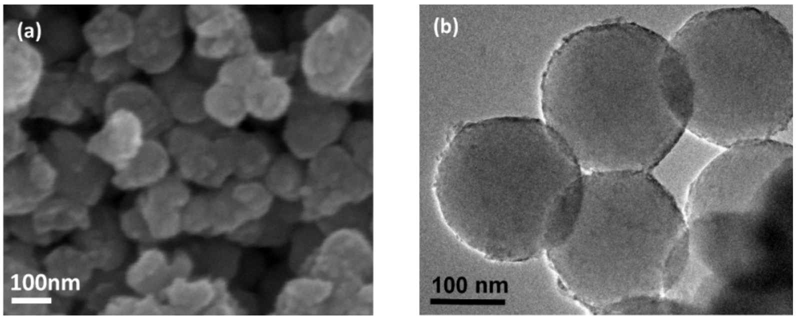

Fig. S1 (a) SEM image of $TiO_2$ spheres. (b) TEM image of $SiO_2$@$TiO_2$ core-shell nanocomposites.

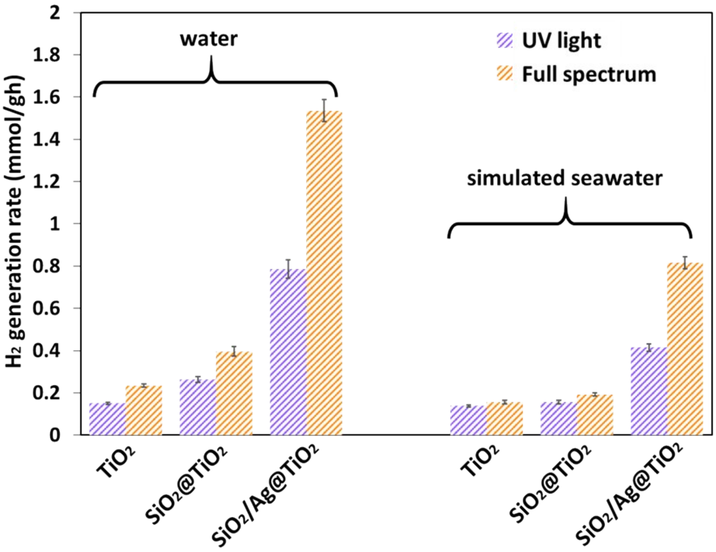

Fig. S2 Hydrogen generation rate of $TiO_2$ spheres, $SiO_2$@$TiO_2$ and $SiO_2$/Ag@$TiO_2$ core-shell nanocomposites in both glycerol-water and glycerol-simulated seawater solution under both UV light and full spectrum irradiation.

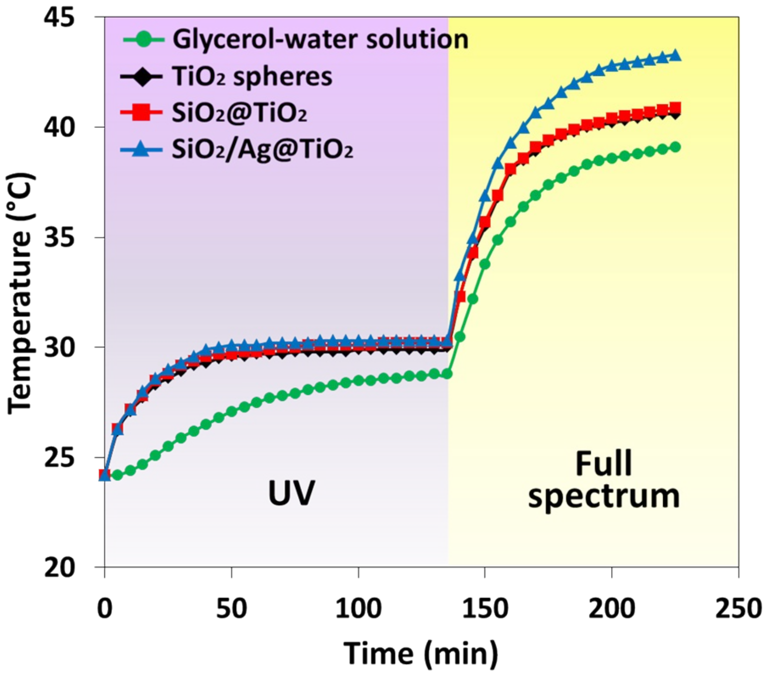

Fig. S3 Temperatures of glycerol-water solution without photocatalysts and with $TiO_2$ spheres, $SiO_2$@$TiO_2$ and $SiO_2$/Ag@$TiO_2$ core-shell nanocomposites under both UV and full spectrum irradiation as a function of time.

2 ml of glycerol sacrificial reagent was dissolved in 8 ml of DI water, to which 5 mg of $SiO_2/Ag@TiO_2$ core-shell composites or 5 mg of $TiO_2$ nanospheres were added. All experiments were carried out in 25 ml quartz vials and illuminated with a UV light source (365 nm) with light intensity of 35.3 mW $cm^{-2}$ for hydrogen generation. A 300 W Xe lamp (Excelitas, PE300BFM) with light intensity of 100 mW $cm^{-2}$ equipped with a 400 nm long-pass filter was used as visible-NIR light source. The vials were purged while immersed in a hot bath of the desired temperature, so as to ensure the vial remains close to 1 atm pressure during the experiment. The headspace in the reaction mixture was syringed drawn (100 μl) to sample the gas composition using gas chromatographer (Shimadzu, GC-2014AT). The quartz vial was kept in a water bath at varying constant temperatures in order to keep the bulk temperature of the reactor constant throughout the experiment (Fig. S4). The vial was first illuminated with UV light in order to obtain the base hydrogen generation rate at the specific temperature. After 1 hour, the Xe light source was switched on concurrently and hydrogen generation rate was measured under full spectrum while keeping the temperature of the quartz vial the same in the water bath. This allows the localized heating effect due to the vis-NIR light to be isolated from the bulk temperature heating, so that its effect on photocatalytic hydrogen generation can be verified.

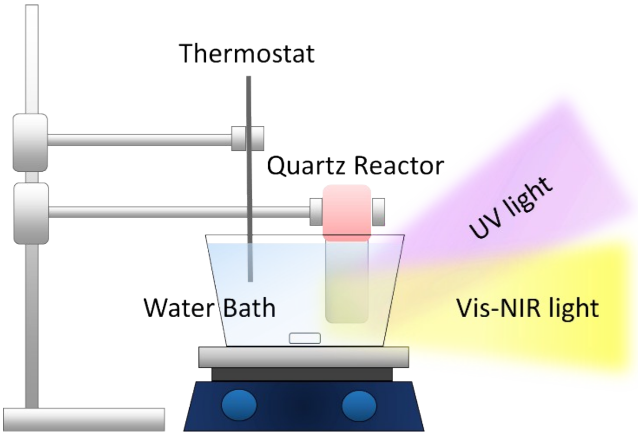

Figure S4: Experimental set-up to isolate the photothermic effect on photocatalytic activity. Do note that both UV and Vis-NIR light sources are directed at the reactor.

It can be seen that for the $SiO_2$/Ag@$TiO_2$ core shell structure, the concurrent illumination of UV and visible-NIR light sources resulted in enhanced $H_2$ generation consistently across all temperatures from 0-90 °C (Fig. S5 a). In contrast, the $TiO_2$ nanospheres show little to no increase in the rate of $H_2$ evolution under the same measurement conditions (Fig. S5 b). This further validates the contribution of photothermic effect leading to enhanced photocatalytic activity of $SiO_2$/Ag@$TiO_2$.

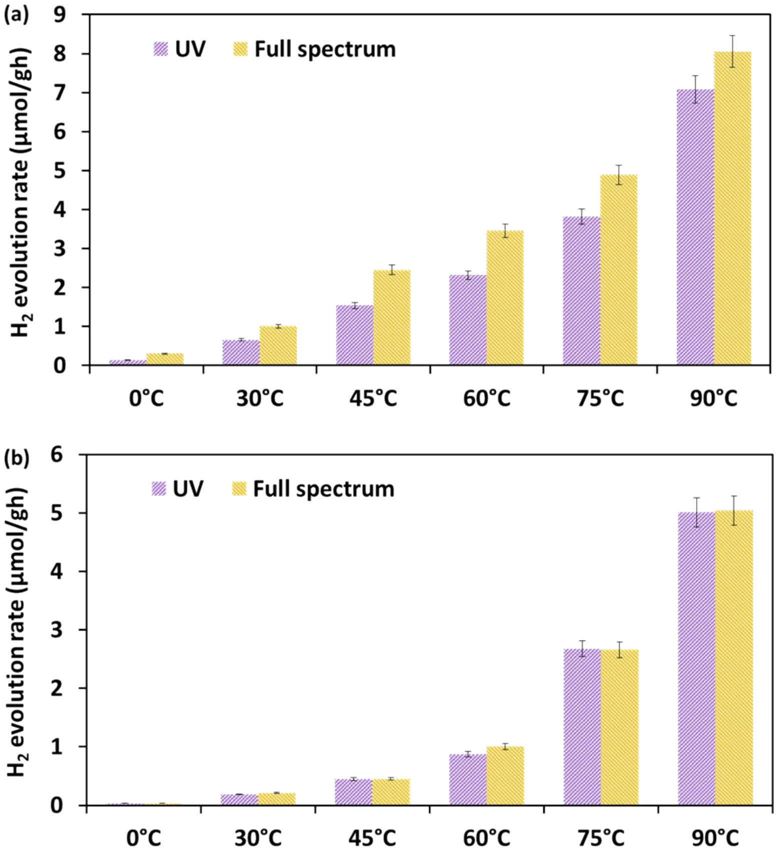

Figure S5: Hydrogen generation rate of (a) $SiO_2$/Ag@$TiO_2$ and (b) $TiO_2$ nanospheres core-shell nanocomposites in glycerol-water solution under both UV light and full spectrum irradiation.

For the localized photothermic characterization through thermal curing of poly-(dimethylsiloxane) (PDMS) (Sylgard 184 silicone elastomer), GaN substrates were first cleaned by immersion in an ultrasonic water bath in acetone, DI water and iso-propanol respectively for 5 min each. The $SiO_2/Ag@TiO_2$ spheres were then deposited on the cleaned GaN substrate by drop-casting its solution and drying at room temperature. After that, a layer of freshly prepared optically transparent PDMS precursor mixed with the thermosensitive curing agent in the ratio of 10:1 was spin-coated onto the substrate. The prepared substrate was illuminated under a 300 W Xe lamp with a cutoff filter ($\geq$400 nm) for 60s, at a distance of 15 cm away from the lamp. After irradiation, the substrate was rinsed twice with hexane to remove any non-cross-linked polymer residuals and then analyzed by SEM.

The localized heating of the $SiO_2/Ag@TiO_2$ spheres leads to polymerization in the immediate surrounding owing to plasmonic photothermic effect. The heat radially spread out to the polymer to form the hemispherical shape of the polymer shell in proximity of the $SiO_2/Ag@TiO_2$ sphere.

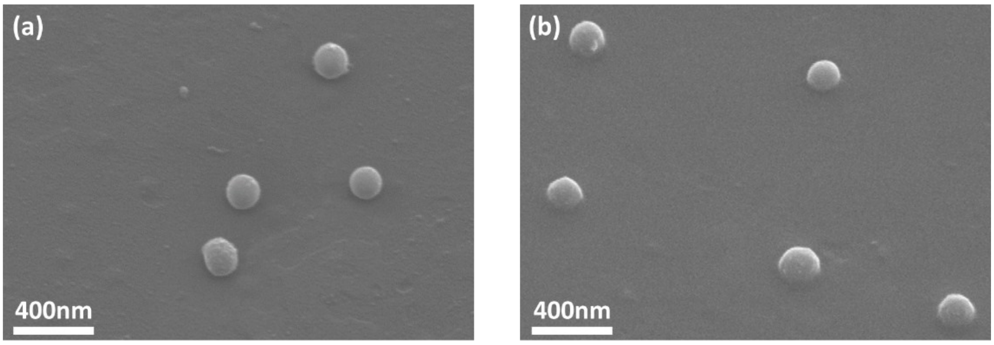

Fig. S6 SEM images of $SiO_2/Ag@TiO_2$ nanocomposites on GaN substrate taken from a 30° angle without PDMS (a) and with PDMS structures formed by thermal curing through localized photothermic effect (b).

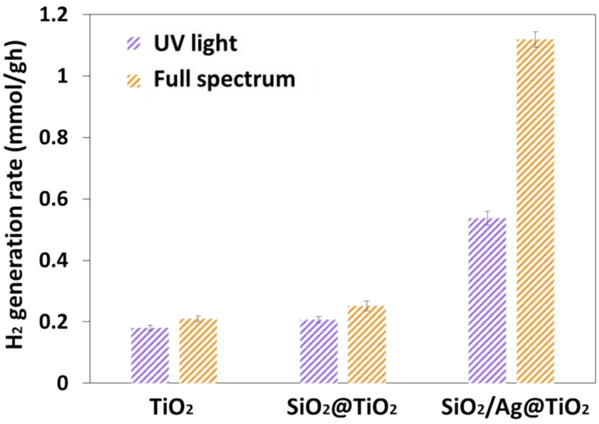

Fig. S7 Hydrogen generation rate of $TiO_2$ spheres, $SiO_2$@$TiO_2$ and $SiO_2$/Ag@$TiO_2$ core-shell nanocomposites in actual seawater under both UV light and full spectrum irradiation.

**Calculation of solar absorptance:**

The performance of the solar thermal collector were characterized by its total solar absorptance. Using Kirchhoff's law, solar absorptance can be expressed in terms of total reflectance, which is the sum of both the specular and diffused reflectance, R (λ, θ) for opaque materials at wavelength λ with incidence angle of light θ as shown in equation (1):[1]

$$\alpha(\theta, \lambda) = 1 - R(\theta, \lambda) \quad (1)$$

Total solar absorptance for a given angle of incidence θ is obtained by weighting the spectral absorptance with the solar spectral irradiance distribution of standard sunlight and integrating over the wavelengths, in which solar radiation reaches the solar thermal collector surface. Equation (2) describes the total solar absorptance, α(θ), of a solar thermal collector for an incident angle of θ

$$\alpha(\theta) = \frac{\int_{\lambda_{min}}^{\lambda_{max}} [1 - R(\theta,\lambda)]A(\theta,\lambda)d\lambda}{\int_{\lambda_{min}}^{\lambda_{max}} A(\lambda)d\lambda} \quad (2)$$

where $\lambda_{min}$, $\lambda_{max}$ are 0.3 μm and 2.5 μm, respectively, and θ is the angle of incidence of light measured from the surface normal of the absorber. A(λ) is the wavelength-dependent solar spectral irradiance. R(θ,λ) is the total reflectance at wavelength λ.[2]

In this experiment, solar reflectance measurements were performed at near normal ($\theta \approx 8°$) angle of incidence using standard spectrophotometers in the wavelength range 0.3-2.5 μm. This means the solar absorptance is characterized at near normal incidence for which the sun is at the zenith angle relative to the solar thermal collector. For oblique incidence, where the sun is at other elevations then the zenith, the near normal solar absorptance must be modified when characterizing solar thermal collector systems.

### †Steam Generation Experiment:

Steam generation through light absorption was carried out by means of simulated concentrated light from a 300 W Xe lamp. The light intensity was kept at 700 mW $cm^{-2}$, comparable to the measured concentration factor of the parabolic trough reflector. Two 25 ml insulated quartz vials were first filled with 10 ml of DI water, and 5 mg of $SiO_2/Ag@TiO_2$ nanocomposite suspension was added to one of the vials. They were then placed separately in front of the Xe lamp with a 12 $cm^2$ window to observe the effect of steam generation under light for 1 h. Under irradiation, it was observed that the quartz vial with only water had a mass loss of 3.99 g, while the vial with the nanocomposites had a mass loss of 6.82 g. This translates to an evaporation rate of 3.33 $L/m^2/h$ and 5.68 $L/m^2/h$ respectively. The results suggests a substantial potential increase in the condensate production with a better reactor design to optimise condensate collection.

1. N. P. Sergeant, M. Agrawal and P. Peumans, Proc. SPIE 7410, Optical Modeling and Measurements for Solar Energy Systems III, 2009.
2. A. Amri, Z. T. Jiang, T. Pryor, C.-Y. Yin and S. Djordjevic, *Renewable Sustainable Energy Rev.*, 2014, **36**, 316-328.